

12TH INTERNATIONAL BRICK/BLOCK Masonry CONFERENCE



Kva

CONSTITUTIVE PROPERTIES OF LIGHTWEIGHT CONCRETE MASONRY

K. V. Høiseth, T. Kvande

¹LECA® Light Expanded Clay Aggregate

²DIANA (Displacement ANALyzer) is a general finite element software environment

ABSTRACT

The present paper deals with the uniaxial stress-strain relationship of lightweight concrete units and masonry. The purpose of the study was to demonstrate the capability to reproduce experimental observations by numerical simulations. In the numerical simulations, the mechanical behaviour was represented by a smeared crack model with a nonlinear softening diagram. The obtained relationship between load and deformation, as well as the crack-pattern and crack-propagation was in good agreement with the experiments. Concerning the stress/deformation relationship, the smeared crack models dependency of the crackband-width has been demonstrated. The study has shown the significance of shear retention in crack-planes even under uniaxial conditions.

Key words: *Lightweight Concrete Masonry, Experimental Testing, Material Modelling, Uniaxial Tension.*

INTRODUCTION

A proceeding doctoral study at NTNU, Faculty of Civil and Environmental Engineering, "Material properties for masonry of lightweight concrete as a constructive material" aims at providing documentation of structural properties and options as basis for product development and improvements in structural utilisation.

In this connection, experimental testing is being performed in order to investigate the mechanical properties of lightweight aggregate concrete units of the LECA¹ type, the properties of the joints between units and the properties of the combined action of units and joints in masonry. The material testing, which concerns stress/strain relationship under various loading conditions, strength parameters, creep and shrinkage, as well as fracture energy, is carried out at TU-Eindhoven.

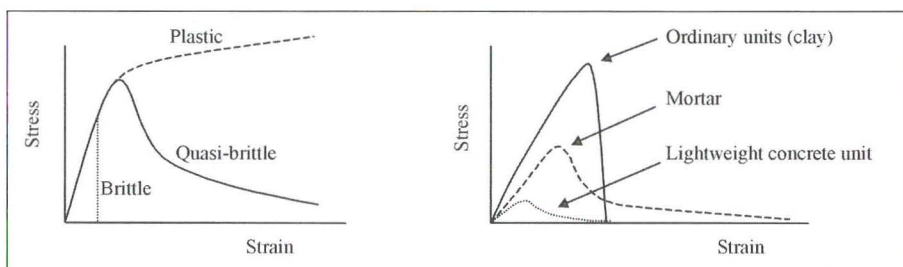
An important part of the study is to adapt the results of the testing to generic material models available in DIANA², which are applicable for structural analysis of masonry. The adapted models will allow analysis of structures with random geometry, -boundary conditions and loadings, with respect to the complete deformation process, from elastic behaviour via cracking to global failure. The models are also necessary for reassessment purposes, or in order to simulate the structural behaviour after the appearance of a local failure, and hence estimate the redundant loadcarrying capacity under service life conditions. In the current project, specifically, the quality of the models will be evaluated by comparing numerical results and experimental observations.

The current paper deals with masonry and units subjected to uniaxial tension. The purpose of the study was to demonstrate the capability of numerical simulations to reproduce the experimental observations (4).

CHARACTERISTIC PROPERTIES

The mechanical behaviour of masonry and of its constituents: units, mortar and the interface between units and mortar shows the characteristics of so-called quasi-brittle materials. When subjected to pure compression, tension or shear, as well

Figure 1. *a) Stress/strain relationship for plastic, brittle and quasi-brittle materials.
b) Relationship for ordinary units, mortars and lightweight concrete units.*



as combined states of stress, the stress/strain relationship follows the schematised curve in Figure 1a. When the peak stress has been reached, additional straining leads to increased bridging of microcracks and hence a softening of the material.

Figure 1b shows a schematised stress/strain relationship for ordinary units compared to the constitutive behaviour of mortar and lightweight concrete units. Due to the relatively high stiffness and strength of ordinary units, both in tension and compression, compared to the values of mortar, the joints and adhesion zone represents the weak links in ordinary masonry. A realistic description of the constitutive behaviour in these areas are therefore important, while the units in most cases will not be subjected to stress levels exceeding the elastic limit.

Concerning lightweight concrete masonry, however, the conditions are opposite, compared to the stiffness and strength of units, the values for mortar is higher. In structural analysis, this implies that also the units must be represented by a material model which accounts for the complete stress/strain relationship, including the softening part.

MATERIAL MODELLING

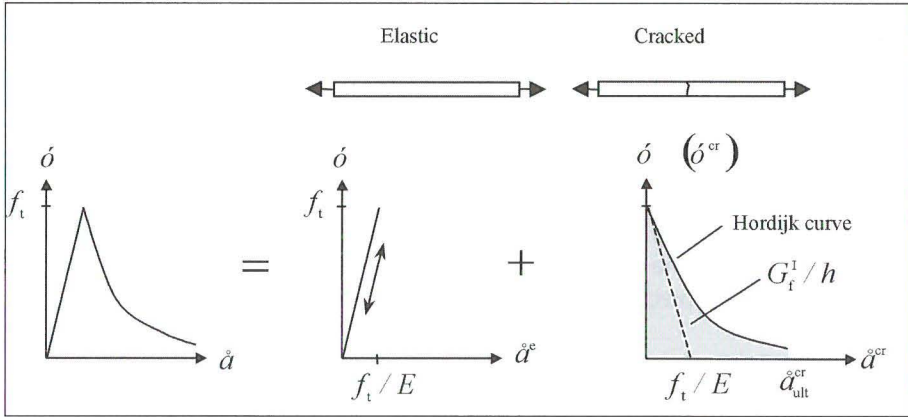
The smeared crack model

Analyses of the tension tests have been performed with a smeared crack model representing the LECA as well as the joint. The smeared crack approach is based on the assumption that the discrete properties of cracks can be distributed over a so-called equivalent length of a continuum. Instead of treating crack widths and sliding between crack planes as displacements, they are included in the strain tensor. In a Finite Element context, this implies that the constitutive behaviour of cracking is being accounted for in the integration points of the elements.

In the current model, this is done by decomposing the strain in an elastic strain component, and a crack strain component. As long as the material is subjected to stresses less than the tensile strength, the mechanical behaviour is linear elastic, according to Hooke's law. A smeared crack is initialised when the maximum principal stress exceeds the tensile strength of the material (mode-I fracture criteria). If the deformation is increased, the capacity of the crack to transfer tension diminish.

A schematised stress/strain relationship of such an event is shown in Figure 2, which illustrates a bar subjected to uniaxial tension (mode-I fracture). At the onset of tension, the bar behaves linearly elastic. When the tensile strength is reached, a crack is initiated in the bar. The elastic strain component is at its maximum, f_t/E , while the crack strain is still zero. From this point on, further stretching leads to a stress reduction as the crack strain increases and the elastic strain decreases. Eventually, the crack will be fully opened without any resistance to transfer tensile stress, the crack strain has reached ϵ_{ult}^{cr} and the elastic strain component is back to zero.

Figure 2. Strain decomposition illustrated by uniaxial tension (Mode-I fracture).



The relationship between the tensile stress and the crack strain is usually referred to as the softening diagram. In the present study, a nonlinear formulation proposed by Hordijk (5) was used. The shape of the softening diagram, which is illustrated in Figure 2, reads:

$$\frac{\sigma}{f_t} = \left(1 + (C_1 \frac{\epsilon^{cr}}{\epsilon_{ult}^{cr}})^3\right) e^{-C_2 \frac{\epsilon^{cr}}{\epsilon_{ult}^{cr}}} - \frac{\epsilon^{cr}}{\epsilon_{ult}^{cr}} (1 + C_1^3) e^{-C_2} \quad (1)$$

$$\epsilon_{ult}^{cr} \approx 5.14 \frac{G_f^I}{f_t}$$

C_1 and C_2 are dimensionless constants, taken as: $C_1=3, C_2=6.93$

It should be noticed that the area under the σ - ϵ_{ult}^{cr} curve is equal to the fracture energy related to mode-I fracture, G_f^I , divided by the so-called equivalent length h . The fracture energy is a material parameter which represents the amount of potential energy required to create one unit of fractured area. Also the equivalent length may be considered a material parameter. In this physical case, the equivalent length represents the thickness of the fracture zone. Fracture in quasi-brittle materials like concrete (LECA) is namely not a completely discrete phenomenon, the fracture zone is an area where microscale cracking take place before an ultimate crack develops. The thickness of this area in front of-, and around the ultimate crack- tip, is approximately 3 times the maximum aggregate size (2).

In smeared crack models, the equivalent length is also known as the crackband-width, and often considered to be an element-related property. Equation (2) shows the relation between the fracture energy and the crackband-width.

$$G_f^I = h \int_{\epsilon_{cr=0}^{cr}} \sigma^{cr} \epsilon^{cr} d\epsilon^{cr} \quad (2)$$

where $h\epsilon^{cr} = w$ (Crack width)

Figure 3 Mesh-objectivity with respect to crackband-width, h .

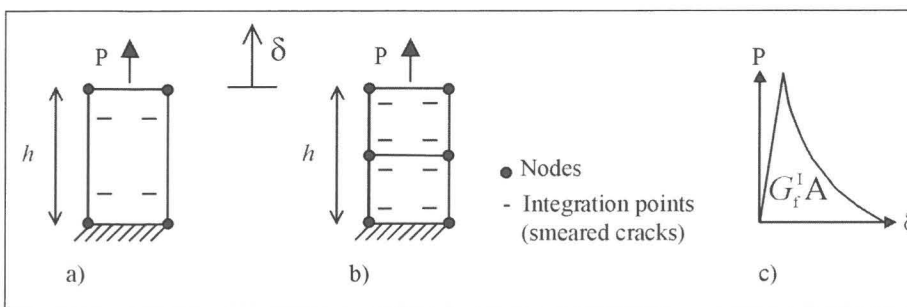


Figure 3a shows a simple test modelled by a single membrane element with 2×2 Gauss integration points. The crackband-width h is taken as the height of the element. The global P/δ curve, and thus also the energy content, is equal to that in Figure 3c. The same result is achieved if the specimen is modelled by two elements, as shown in Figure 3b. This is however only true if the crackband-width h is kept equal in both cases. If the crackband-width is taken equal to the element-height, the energy content in the latter case, Figure 3b, would be twice as large as that of Figure 3a.

The example illustrates a deficiency of the smeared crack approach, namely that the solutions need not be objective with respect to the element mesh resolution. The choice of h must therefore be adapted to the crackband-width, which is obtained by numerical analysis and which can be judged as representing discrete cracks.

Under general and unproportional loading conditions, the directions of the principal stresses change. When cracking has been initiated, this implies that a shear deformation will appear parallel to the crack plane. The shear resistance on a crack plane will of course be less than in the uncracked state. In the present study, a linear relation between shear stress and – strain is maintained also after cracking, however the shear-modulus on the crack-plane is reduced by a constant shear retention factor β .

The smeared crack model allows multiple cracks to develop in each integration point. After the first crack has been initiated, subsequent cracks in an integration point are formed when the following criteria are satisfied simultaneously:

- The principal tensile stress is larger than the tensile strength.
- The angle between existing cracks and the direction of the principal tensile stress exceeds the value of a given threshold value.

A detailed description of this multidirectional smeared crack model as well as the implementation of the model in a Finite Element context is given in (1) and (3).

MATERIAL PROPERTIES

The material properties were taken from the experiments (4), and it was the mean values which were used, see Table 1. Young's modulus refers to the initial tangent modulus.

NONLINEAR ANALYSIS OF UNIT

Geometric model, boundary conditions and loading

The test specimen was modelled under the assumption of two-dimensional plane stress conditions. Due to symmetry about the vertical centre-line, merely half the test specimen was represented, see Figure 4. The model was assembled by eight-node quadrilateral isoparametric membrane elements (CQ16M), with a 2x2 Gauss integration scheme.

In the experimental testing, the top and bottom face of the specimens were glued to stiff steel platens. The nodes at the top and bottom of the model were therefore fixed in the horizontal direction. Symmetric conditions were achieved by fixing the nodes along the line of symmetry in the horizontal direction. In line with the experiments, the nodes in the bottom of the model were fixed also in the vertical direction.

The length between the points P and S corresponds with the measuring length of the LVDT's which were used in the experiments.

RESULTS

Initial analysis had indicated that a global, fully opened crack would develop through a horizontal row of integration points. With the applied 2x2 integration rule, the crackband-width was therefore taken equal to half the element height.

Table 1. Material properties until testing (4)

	Young's	Poisson's ratio	Tensile	Shear	Fracture Energy	Crackband
	modulus	ν	strength	retention	G_f (Nm/m ²)	width
	E (Mpa)		f_t (Mpa)	β		h (m)
LECA	3000	0.2	0.5	0.03	30	0.0015

Table 2. Material properties masonry testing (4)

	Young's	Poisson's ratio	Tensile	Shear	Fracture Energy	Crackband
	modulus	ν	strength	retention	G_f (Nm/m ²)	width
	E (Mpa)		f_t (Mpa)	β		h (m)
LECA	3000	0.2	0.5	0.03	30	0.0015
Joint	1313	0.2	0.25	1.0 (0.03)	11	0.0015

Figure 4. FE-model of tension tests.

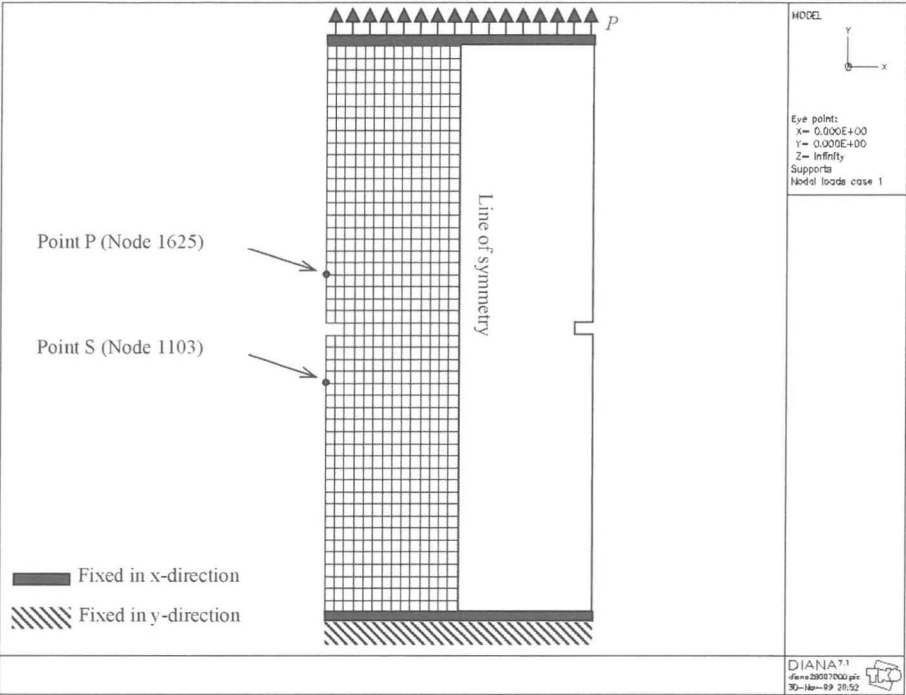


Figure 5 shows the relationship between the load and the extension of the distance between the points P and S. The curve obtained in the analysis is compared to a curve representing an average of the experimental results, fitted to the softening diagram of Hordijk, see (4). It should be noticed that the fracture energy, both in the smeared crack model as well as in the empirical expression, was entered with the same value. Hence, one should expect the area under the curves to be fairly equal. The tensile stress in the diagram represents the externally applied load divided by the cross-sectional area through the notches of the specimen.

The fully developed crack pattern is illustrated in Figure 6, which also shows a close view of the crack-propagation in relation to the stress level. Due to stress concentration, cracking is initiated in the integration points nearest to the notch, with a crack plane normal to the direction of the principal stress. Because of the notch, the direction of the principal stress is not vertical. A closed-form solution under linear elastic conditions would have given an infinite principal stress in the corners of the notch. This is not achieved by the discretization inherent in the Finite Element method, however also in the numerical results the stress concentration in the corners of the notch was significant. The direction of the initial crack planes was in agreement with observations made during testing.

Figure 6 shows that, as the cracking propagates towards the interior, the angle of the crack-planes become horizontal, and the direction of the principal stresses in-

Figure 5. Relationship between load and displacement (P-S extension, see Figure 4).

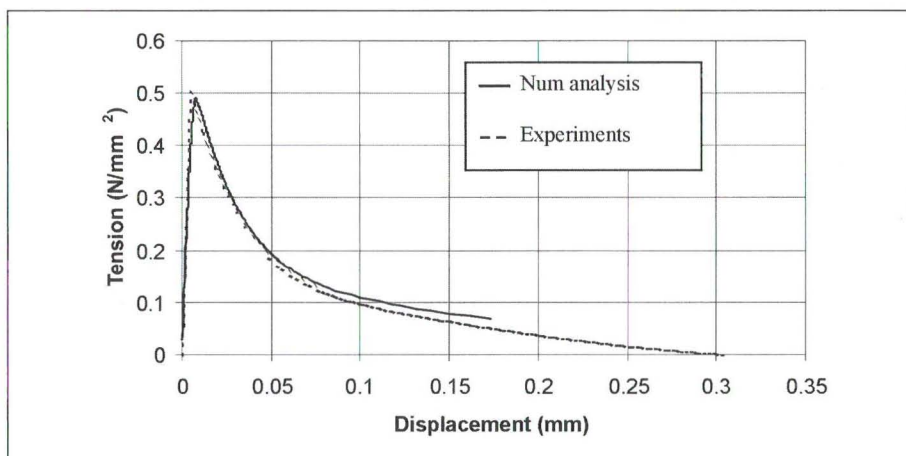
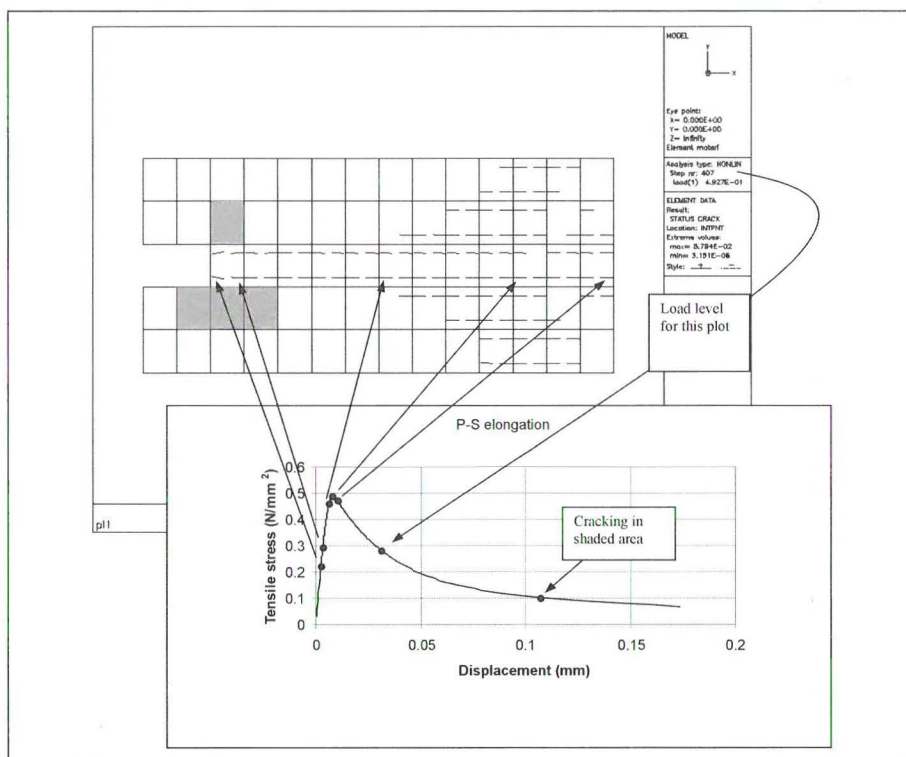


Figure 6. Crack propagation.



creasingly vertical. This explains the crack-branching above and under the main horizontal crack, in the area close to centre of the specimen. After the crack-pattern was established, these branches closed, and a global crack developed through the cross section along the lower line of integration points in the elements ex-

tending horizontally from the notch. It should be emphasised that the analysis was unstable at the point of maximum load, when the crack pattern was about to be fully developed, ie run through the entire cross-section. At this stage, the analysis was performed with arc-length control, with very small load-steps. That the main crack opened merely along the lower row of integration points and not the upper, or both, must therefore be regarded as a numerical coincidence.

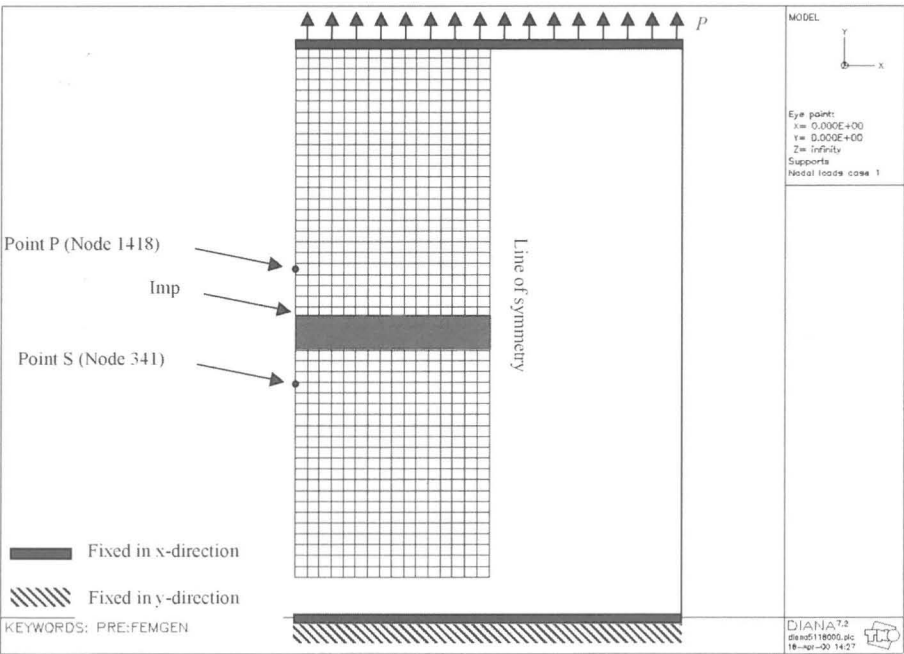
An additional analysis was performed, where the nonlinear formulation of Hordijk was replaced by a linear softening diagram. This produced a similar crack-pattern, with the same fracture energy, however the final deformation after unloading was obviously less.

NONLINEAR ANALYSIS OF MASONRY

Geometric model, boundary conditions and loading

The test specimen was modelled under the assumption of two-dimensional plane stress conditions. Due to symmetry about the vertical centre-line, merely half the test specimen was represented, see Figure 7. The model was assembled by eight-node quadrilateral isoparametric membrane elements (CQ16M), with a 2x2 Gauss integration scheme.

Figure 7. FE-model of masonry test.



In the experimental testing, the top and bottom face of the specimens were glued to stiff steel platens. The nodes at the top and bottom of the model were therefore fixed in the horizontal direction. Symmetric conditions were achieved by fixing the nodes along the line of symmetry in the horizontal direction. In line with the experiments, the nodes in the bottom of the model were fixed also in the vertical direction.

The top-row of elements were subjected to consistent edge loading with a constant distribution.

The length between the points P and S corresponds with the measuring length of the LVDT's, which were used in the experiments.

RESULTS

The extension between the points P and S in relation to the loading, is given by the curve denoted "Num analysis" in Figure 8. The curve "Experiments" belongs to an average of the experimental results, inserted in Equation (1).

The crack pattern at the end of the analysis is given in Figure 9. Cracking is initiated in centre of the joint, and in the middle of the specimen. This is due to the different material properties of LECA and joint, which implies that the principal stress in the middle of the specimen becomes slightly higher than at the surface. From this area, the cracking propagates horizontally towards the surface. At the end of loading, a global and fully opened crack run through a horizontal row of integration points, while in the adjacent elements, crack-closure have taken place.

Figure 8. Relationship between load and displacement (P-S extension).

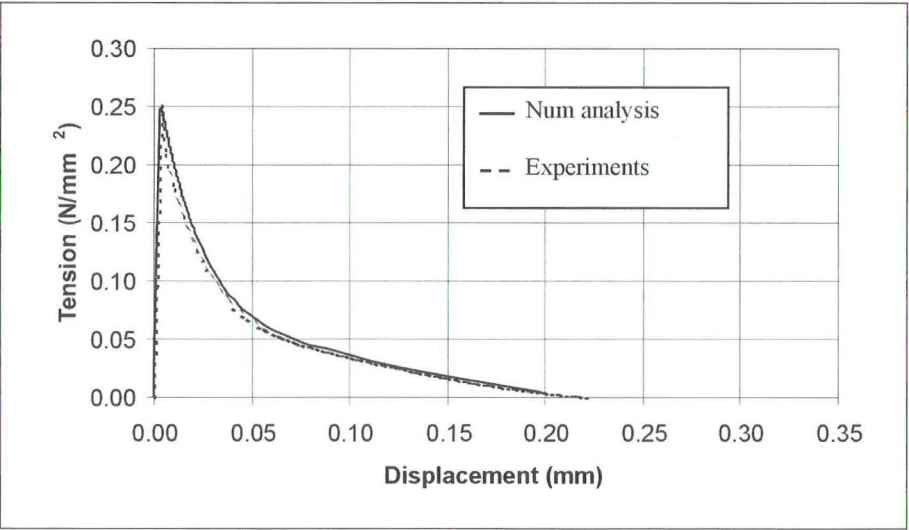
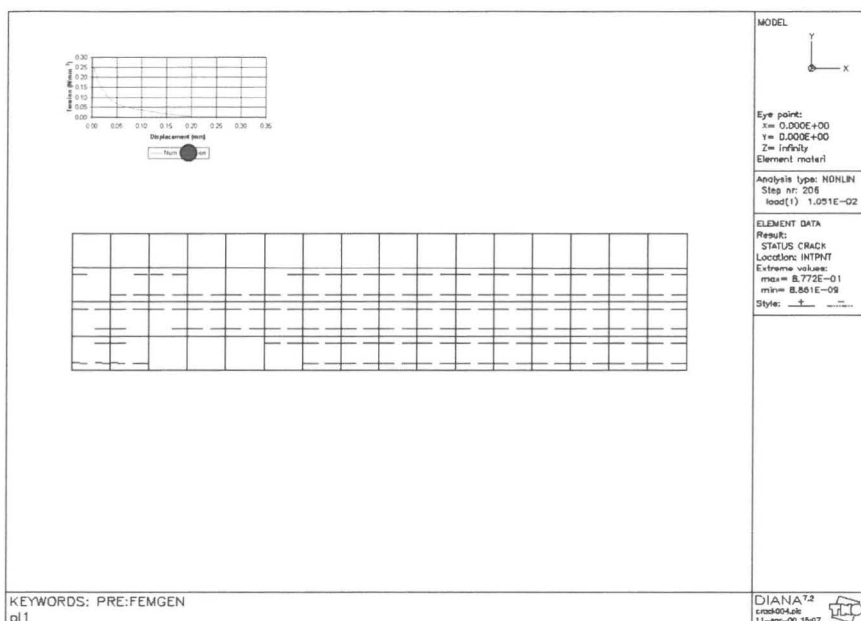


Figure 9. Crack pattern at the end of analysis.



The localisation of the crack-band in combination with the anticipated crack-band width, which was taken equal to the influence length of one integration point (Table 1), explains the close agreement between the deformation curves in Figure 8.

As a first approach, the analysis was performed with a low shear retention factor, $\beta=0.03$. This produced a horizontal, but wave-like global crack, which gave unrealistic large shear deformations in the joint during unloading.

During casting and curing of the specimens, it was observed that due to seep and drying creep of mortar, contact was lost between joint and unit along the circumference of the joint. The result was a small notch, which may act as a crack initiator. In order to demonstrate this effect, numerical analyses were performed on a model with a small imperfection, by means of removing the contact between the outermost two nodes at the surface of the specimen between the upper unit and the joint, see the area denoted Imp in Figure 7. Due to the stress concentration, this produced an initial crack, with a propagation highly dependent on the applied shear retention. With full shear retention, cracking even extended somewhat into the units.

CONCLUSIONS

From the experiments, there are two observations particularly useful for evaluation of the numerical analyses: the cracking and the relationship between stress (loading) and deformation.

The analyses of units showed that cracking was initiated in the integration points nearest to the notch. The normal to the crack planes pointed towards the corner of the notch, which corresponds with the direction of the principal tensile stress in this area. With a linear softening diagram, as well as with the Hordijk formulation, the cracking propagated horizontally. Close to the centre of the specimen, crack branching occurred due to increasingly uniaxial stress distribution. After a fully developed crack pattern, however, the crack opening took place in the extension of the notch. This is in agreement with experimentally observed behaviour. It should be noticed that also in the experiments, frequently two cracks were initiated in the corner of the notches (4).

Concerning the stress/deformation relationship, the smeared crack models dependency of the crackband-width has been demonstrated. Provided a realistic crackband-width is used, both softening diagrams gave a fracture energy close to those which were measured in the experiments. The Hordijk softening diagram is however more in line with the mechanical behaviour of quasi-brittle materials like LECA, and the deformations were therefore also closer to the experimental results.

In the experiments with masonry specimens, the test results showed that complete fracture occurred in the interface between units and joint.

The nonlinear analysis with an ideal connection between units and joint, and with full shear retention, produced a complete horizontal fracture in the middle of the joint. This discrepancy between observed and numerical results indicates a higher stiffness and strength in the middle of a joint than in the interface area. In the analysis, average properties were used.

Due to the horizontal crack-band achieved in the analysis, which was in agreement with the anticipated crack-band width, the load-deformation relationship was very close to the measured one.

Seep and drying shrinkage along the surface of joints may produce stress-concentrations and hence initiate cracking in the interface between units and joint. This has been demonstrated by numerical analyses. However, both with full shear retention and almost no shear resistance in crack-planes, the crack propagation took place in the middle of the joint. Again, this is probably due to higher stiffness and strength in the middle of a joint than at the interface.

The analyses have shown that, even under uniaxial conditions, shear retention is an important parameter with respect to the development and propagation of cracks. With full shear retention, cracking even extended somewhat into the units. Taking into consideration that the stiffness and strength of the interface between unit and joint are comparable with the stiffness and strength of units, this could indicate that lightweight concrete masonry may be considered as homogeneous material. The implications of such an approximation need however to be quantified.

ACKNOWLEDGEMENTS

The present work was initiated by Oddvar Hyrve, Research Director in Norsk Le-ca AS. He soon involved the masonry guild at the Faculty and the Norwegian Masonry Centre, which has been an excellent forum for discussions about numerical analysis of masonry structures. Their funding of the present study is highly appreciated.

At the Peter van Musschenbroek Laboratory of TU-Eindhoven, a number of test-facilities for investigation of the mechanical behaviour of masonry have been developed over the years. This equipment, in combination with the extensive competence of the scientific staff at the Faculty of Architecture, made the experimental investigations possible.

REFERENCES

1. *Diana, User's Manual release 7– Nonlinear Analysis*, TNO Building and Construction Research, 1998.
2. Gylltoft, K.: *Fracture Mechanics Models for Fatigue in Concrete Structures*, Doctoral Thesis 1983:25D, University of Luleå, Division of Structural Engineering.
3. Rots, J. G.: *Computational Modeling of Concrete Fracture*, Doctoral Thesis, Delft University of Technology, Civil Engineering Department, 1988.
4. Kvande, T.: *Deformation Controlled Tensile Tests on Masonry of LECA*, Working report 6, October 1999.
5. Hordijk, D. A.: *Tensile and Tensile Fatigue Behaviour of Concrete; Experiments. Modelling and Analyses*, Heron Vol. 37 No. 1, 1992.
6. Høiseth, K. V.: *Material Modelling of Lightweight Concrete Masonry Units (LECA) – Uniaxial Tension*, R-15-99, NTNU, Dep of Struct Eng, 1999.
7. Høiseth, K. V.: *Material Modelling of Lightweight Concrete Masonry (LECA) – Uniaxial Tension of Masonry*, R-3-00, NTNU, Dep of Struct Eng, 2000.

